Tissue distribution of radioiodinated FAUC113

Assessment of a pyrazolo(1,5-*a*)pyridine based dopamine D4 receptor radioligand candidate

O. Prante[1], C. Hocke[1], S. Löber[2], H. Hübner[2], P. Gmeiner[2], T. Kuwert[1]
[1]Laboratory of Molecular Imaging, Clinic of Nuclear Medicine (Head: Prof. Dr. T. Kuwert),
[2]Department of Medicinal Chemistry (Head: Prof. Dr. P. Gmeiner), Friedrich-Alexander University Erlangen, Germany

Bioverteilung von Radioiod-markiertem FAUC 113: Bewertung eines potenziellen Radioliganden für den Dopamin D4-Rezeptor mit Pyrazolo(1,5-a)-pyridin-Grundkörper

Keywords
D4 receptor, radioligand, autoradiography

Summary
Aim: Disturbances of the D4 receptor subtype have been implicated in the genesis of a broad range of psychiatric disorders. In order to assess the suitability of a radioiodinated analogue of the D4-selective ligand FAUC 113 for tracer studies in vivo, we investigated the in-vivo stability, biodistribution and brain-uptake of 7-^{131}I-FAUC 113 in Sprague-Dawley rats. **Methods:** Radiolabelling was carried out with high radiochemical yield and specific activity. After intravenous injection, blood and tissue samples, taken at designated time intervals, were collected for analysis. Analyses of metabolites were performed by radio-hplc and radio-tlc. For in-vivo evaluation, sagittal cryo-sections of the rat brain were investigated by in-vitro and ex-vivo autoradiography on a μ-Imager system. **Results:** 7-^{131}I-FAUC 113 was rapidly cleared from blood. Highest uptake was observed in kidney (0.603 ± 0.047% ID/g, n = 4) and liver (0.357 ± 0.070% ID/g, n = 4) at 10 min p.i.; 7-^{131}I-FAUC 113 displayed rapid uptake (0.21-0.26% ID/g) and fast clearance in various brain regions consistent with the determined logP-value of 2.36 ± 0.15 (n = 4). In-vivo stability of 7-^{131}I-FAUC 113 was confirmed in the frontal cortex (> 95%). Ex-vivo autoradiography revealed a frontal cortex-to-cerebellum ratio of 1.57 ± 0.13 at 10 min p.i. (n = 6). Coinjection with L-750667 could not suppress any putative specific binding of 7-^{131}I-FAUC 113. In-vitro autoradiography using authentic 7-iodo-FAUC 113 or L-750667 failed to cause significant displacement of the radioligand. **Conclusions:** Radioiodinated FAUC 113 does not allow imaging of D4 receptors in the rat brain in vivo nor in vitro. Further work should aim at the development of selective dopamine D4 radioligands with improved tracer characteristics, such as receptor affinity and subtype selectivity, specific activity or blood-brain-barrier permeability.

Nuklearmedizin 2006; 45: 41–8

Schlüsselwörter
D4-Rezeptor, Radioligand, Autoradiographie

Zusammenfassung
Ziel: Für eine Vielzahl psychiatrischer Erkrankungen wird eine Implikation des Dopamin-D4-Rezeptorsubtyps diskutiert. Um die Eignung eines radioiodierten Analogons des D4-selektiven Liganden FAUC 113 für Tracerstudien in vivo zu beurteilen, haben wir die in-vivo-Stabilität, Bioverteilung sowie die Hirnaufnahme von 7-^{131}I-FAUC 113 in Sprague-Dawley-Ratten untersucht. **Methoden:** Die Radiomarkierung lieferte den Tracer in hoher radiochemischer Ausbeute und spezifischer Aktivität. Nach intravenöser Injektion wurden die zu bestimmten Zeitpunkten entnommenen Blut- und Gewebeproben zur Radio-HPLC/Radio-DC Metabolitenanalyse gesammelt. Für die in-vivo Evaluierung wurden sagittale Kryo-Gewebeschnitte des Rattenhirns mit Hilfe der in-vitro- und ex-vivo-Autoradiographie an einem μ-Imager untersucht. **Ergebnisse:** 7-^{131}I-FAUC 113 wurde schnell aus dem Blut ausgeschieden. Die höchste Aufnahme wurde in der Niere (0.603 ± 0.047% ID/g, n = 4) und Leber (0.357 ± 0.070% ID/g, n = 4) 10 min p.i. beobachtet. 7-^{131}I-FAUC 113 zeigte in verschiedenen Hirnregionen eine schnelle Aufnahme (0.21-0.26% ID/g) sowie Auswaschung. Dies stimmt mit dem ermittelten LogP-Wert von 2.36 ± 0.15 (n = 4) überein. Die in-vivo-Stabilität von 7-^{131}I-FAUC 113 im frontalen Cortex wurde bestätigt (> 95%). Die ex-vivo Autoradiographie zeigte ein Cortex/Cerebellum-Verhältnis von 1.57 ± 0.13, 10 min p.i. (n = 6). Eine Coinjektion mit L-750667 konnte die vermeintlich spezifische Bindung von 7-^{131}I-FAUC 113 im Gehirn nicht unterdrücken. In der in-vitro-Autoradiographie unter Verwendung von 7-iodo-FAUC 113 oder L-750667 erfolgte keine signifikante Deplazierung des Radioliganden. **Schlussfolgerung:** Das radioiodierte FAUC 113 erlaubt in vivo sowie in vitro keine Darstellung des D4-Rezeptors im Rattenhirn. Weiterführende Studien sollten auf die Entwicklung von D4-selektiven Radioliganden mit verbesserten Eigenschaften, wie Rezeptoraffinität und Subtypselektivität, spezifische Aktivität oder Blut-Hirn-Schranken-Durchgängigkeit, abzielen.

The dopamine D4 receptor subtype was cloned (34) and characterized by receptor autoradiography of knock-out mice (6) or immunohistochemistry using receptor-specific antibodies (1, 7, 24). Its precise function and exact distribution in the central nervous system are of great interest. Alterations and disturbances of the D4 receptor were implicated in the genesis and treatment of a broad range of neurobehavioral and psychiatric disorders such as novelty seeking, attention-deficit hyperactivity disorder and schizophrenia (26, 35). A higher density of D4 receptors was found in postmortem brain tissue of schizophrenic patients (32); however, this was not supported by other studies (9, 31). These discrepant findings could be explained by the lack of a selective D4 receptor radioligand with high affinity and selectivity to other dopamine receptors. As yet, dopamine D4 receptor concentrations in vitro can only be determined by indirect binding studies, in which the number of binding sites defined with ^{3}H-raclopride (D2/D3 antagonist) are substracted from total binding (^{3}H-nemonapride) (13, 32). However, recent progress has been made by the synthesis of the first selective tritiated D4 agonist as a radioligand to more accurately characterize competitive binding for agonists at the D4 receptor (22).

Moreover, the lack of D4 receptor selective radioligands suitable for in-vivo imaging techniques especially hampers the non-invasive investigation of neurotransmission by single photon emission tomography (SPET) or positron emission tomography (PET). These methodologies serve as high-performance imaging tools in nuclear medicine for understanding the

Received: May 12, 2005; in revised form: July 14, 2005

neurochemical basis and pathology of neuropsychiatric diseases (2). Several reports concern ^{18}F- and ^{11}C-labelled ligands for the exploration of D4 receptor density in vivo by PET including ^{11}C-SDZ GLC 756 (3), methoxybenzamide derivatives (15, 36), SB-235753 (4, 21) or ^{18}F- and ^{123}I-labelled pyrrolo-2,3-*b*-pyridines (8, 27, 33). However, none of these radioligands has been proven suitable, because of poor specificity in vivo or undesirable pharmacological properties. Thus, data on the apparently low D4 receptor densities in the brain are scarce and were reported only in analyses using in-situ hybridization establishing receptor expression in the prefrontal cortex and hippocampus (17). Furthermore, using autoradiography with ^{3}H-NGD 94–1 B_{max}-values ranging from 9–30 fmol/mg in distinct brain regions were reported (14, 30).

As a part of our drug discovery and SAR investigations on selective dopamine D4 receptor ligands (11, 16, 19, 20), we developed FAUC 113 as a high affinity dopamine D4 receptor ligand with superior subtype selectivity when compared to the corresponding indole derivative (18). Moreover, radioiodination of the lead compound FAUC 113 in 7-position lead to the corresponding 3-[4-(4-chlorophenyl)piperazin-1-yl]methyl-7-^{131}I-iodopyrazolo(1,5-*a*)pyridine (7-^{131}I-FAUC 113) under retention of high D4 receptor affinity (K_i=2.6 nmol/l) and subtype selectivity in vitro (Fig. 1) (29).

The aim of the present study was the investigation of biodistribution, in-vivo stability and brain uptake patterns of 7-^{131}I-FAUC 113 in order to assess the in-vivo properties of this radioligand. We focused on the determination of brain uptake specificity of 7-^{131}I-FAUC 113 by the use of in-vitro and ex-vivo autoradiography.

Animals, material, methods

Na^{131}I, product code IBSSO, was obtained from Amersham (Braunschweig, Germany). Analytical grade chemicals and reagents were purchased from Sigma-Aldirch (Deisenhofen, Germany) or Research Biochemicals International (RBI, Sigma). Phosphate buffered saline (PBS), EDTA and Tween 20 were purchased from Invitrogen (Gibco, Karlsruhe, Germany). Radio-thin layer chromatography (radio-TLC) was carried out on silica gel-coated plates (SIL 300, Macherey-Nagel, Düren, Germany). Radio-TLC was detected and analysed by electronic autoradiography (Instant Imager™, Canberra Packard). Analytical radio-high performance liquid chromatography (radio-HPLC) was performed on the following system: HPLC Hewlett Packard (HP 1100) with quarternary pump and variable wavelength detector (254nm) connected to radio-HPLC-detector D505TR (Canberra Packard).

Computer analysis of HPLC data was performed with FLO-One software (Canberra Packard). Radioactive tissue samples were counted using a NaI(Tl) szintillation counter (Caprac, Capintec). Autoradiography and white-light imaging of brain slices was performed on the real-time µ-Imager system (Biospace Instruments, France).

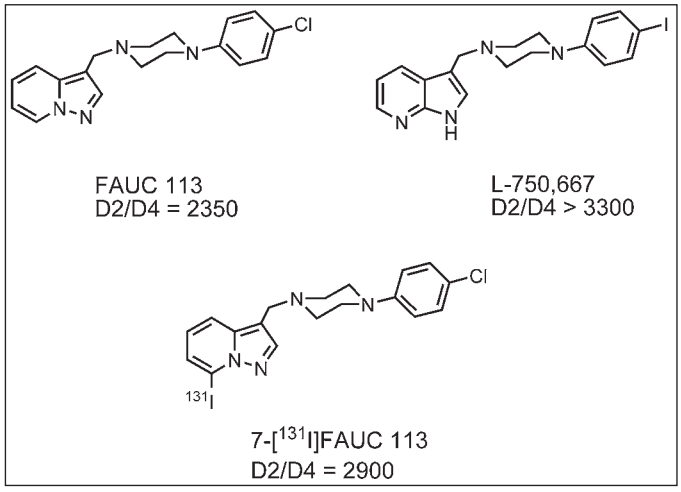

Fig. 1
High-affinity ligands for the D4 receptor: L-750667 (K_i=0.51 nmol/l; 12), FAUC 113 (K_i=2.0 nmol/l; 18) as a lead compound for the radioligand 7-^{131}I-FAUC 113 (K_i=2.6 nmol/l; 29).

Animals

All experiments were conducted according to protocols approved by the local Animal Protection Authorities (Regierung Mittelfranken, Germany, No. 621-2531. 31-16/01). Female Sprague-Dawley rats (200-240 g) were housed in individual cages in a temperature- and air-controlled room with free access to food and water. Animals were maintained on a 12-h light/dark cycle.

Radiochemical synthesis and determination of specific activity

3-(4-(4-chlorophenyl)-piperazin-1-yl)methyl-7-^{131}I-iodopyrazolo(1,5*a*)-pyridine (7-^{131}I-FAUC 113)

Radiochemical synthesis of 7-^{131}I-FAUC 113 was performed by iododestannylation of the 7-tributylstannyl substituted precursor as described previously (29). Ethanol (70%) was used to elute the radioligand from the solid phase (Sep-Pak™ C-18 plus-cartridge, Waters) to obtain a radiochemical purity of 98% (radio-HPLC, radio-TLC: R_f=0.35 (CH_2Cl_2/MeOH; 95:5, v/v). After evaporation of the solvent 7-^{131}I-FAUC 113 was dissolved in phosphate buffered saline (PBS, Gibco) containing 0.01% Tween 20. This solution was used for further animal experiments or in vitro autoradiography. Starting from 30-55 MBq Na^{131}I the radiochemical yield of 7-^{131}I-FAUC 113 was 35% and the specific activity was determined to be >2.6 x10^{10} Bq/µmol by radio-HPLC using a HP-RP-8 Eclipse column (125x4 mm, methanol/0.1 mol/l ammonium formate; 70:30, v/v, pH 6.8; 0.6 ml/min, k'=3.8). The UV absorbance at 254 nm of authentic 3-(4-(4-chlorophenyl)-piperazin-1-yl) methyl-7-^{131}I-pyrazolo(1,5*a*)-pyridine (7-^{131}I-FAUC 113; 29) was used as a reference signal to determine the specific activity of 7-^{131}I-FAUC 113 with a known

radioactivity considering the sensitivity limit of UV-detection (0.4 nmol).

Determination of partition coefficient (logP)

The lipophilicity of 7-[^{131}I]FAUC 113 was assessed by determination of the water-octanol partition coefficient following the procedure of Holschbach et al. (10). After solvent evaporation 7-^{131}I-FAUC 113 was dissolved in 1.0 ml n-octanol saturated with 50 mmol/l Tris-HCl (pH 7.4). The phases were vigorously mixed for 15 min after addition of 1.0 ml 50 mmol/l Tris-HCl (pH 7.4). The solvent phases were seperated with centrifugation at 3000 rpm for 8 min and aliquots of each phase (20 µl, n=3) were used for radioactivity counting. Repeatedly, a defined volume of the octanol phase (100-500 µl) was re-extracted with the same volume of fresh 50 mmol/l Tris-HCl (pH 7.4). Radioactivity determinations of aliquots of each phase (20 µl, n=3) were carried out until the ratio of counts ($cpm_{octanol}/cpm_{buffer}$) was found to be invariant. A constant partition coefficient was reached at least after two re-extraction procedures. The logP-value of 7-^{131}I-FAUC 113 was 2.36±0.15 (n=4), as determined by four independent experiments:

$$logP = \log(cpm_{octanol}/cpm_{buffer}).$$

In-vitro autoradiography

Female Sprague-Dawley rats weighing 200-240 g were sacrificed by decapitation (without anesthesia). Brains were removed and frozen in cooled hexane at -70°C. Sagittal sections of 20 µm were cut on a cryostat microtome (HM550, Microm, Germany) and thaw-mounted on covered glass slides (Histobond®, Marienfeld GmbH, Germany). The brain slices were carefully dried at room temperature and pre-incubated for 5 min in 50 mmol/l Tris-HCl buffer (pH 7.4) containing 120 mmol/l NaCl, 1 mmol/l EDTA, 5 mmol/l $MgCl_2$. Pre-incubation was repeated once and the sections were incubated at room temperature for 60 min in assay buffer (120 mmol/l NaCl, 1 mmol/l EDTA, 5 mmol/l $MgCl_2$) containing 4 MBq 7-^{131}I-FAUC 113 with or without the following ligands: 1,3-di-*o*-tolylguanidine (DTG, 0.5 µmol/l, sigma receptor agonist), pindolol (0.1 µmol/l, serotonin antagonist), L-750,667 (5µmol/l, D4 receptor antagonist ;12) and 7-iodo-FAUC 113 (5µmol/l). Slides were washed two times for 5 min in fresh ice-cold assay buffer and dipped briefly in ice-cold distilled water. Sections were dried under a stream of air and then used for autoradiography (µ-Imager, Biospace).

Blood and tissue distribution of 7-^{131}I-FAUC 113

The biodistribution of 7-^{131}I-FAUC 113 was determined in female Sprague-Dawley rats weighing 200-240 g. 0.9-2.4 MBq 7-^{131}I-FAUC 113 in 50 µl were injected through the tail vein. Three additional animals were injected with 14-20 MBq 7-^{131}I-FAUC 113 in 100 µl (35-50 GBq/µmol) in order to assess the dependence of the amount of radiolabelled ligand on regional brain uptake values. Rats were sacrificed by rapid decapitation (without anesthesia) after designated periods (5, 10, 20 and 40 min). Blood and tissue samples were rapidly removed, measured for radioactivity and weighed. Experiments were conducted on groups of at least three rats per time point, with results expressed as the % of injected dose per gram of wet tissue (%ID/g). For blocking studies, rats received a tail-vein coinjection of 7-^{131}I-FAUC 113 in 50-100 µl PBS containing 1 mg/kg L-750,667.

Analyses of metabolites in rat tissue samples

The determination of radioactive metabolites of 7-^{131}I-FAUC 113 was carried out using blood samples (10 min and 20 min p.i.) and tissue samples of thyroid, frontal cortex and liver obtained at 20 min post-injection unless otherwise indicated. 50-100 mg of tissue were extracted with 900 µl cold methanol/dichloromethane (50:50, v/v) and homogenized with a sonifier. The solution was centrifuged at 5000g for 10 min and the supernatant was used for radio-TLC (CH_2Cl_2/MeOH; 95:5, v/v) or an aliquot (100 µl) was evaporated to dryness and injected into the radio-HPLC (HP-RP-8 column, 125x4mm, methanol/0.1 mol/l ammonium formate; 70:30, v/v, pH 6.8; 0.6 ml/min). The eluate was monitored for radioactivity and UV absorbance at 254nm. Analytical amounts of authentic 7-iodo-FAUC 113 were added to the samples to prove the identity of non-metabolized radioactive 7-^{131}I-FAUC 113.

Ex-vivo autoradiography of brain slices

Regional brain uptake of 7-^{131}I-FAUC 113 was visualized by autoradiography of rat brain slices, usually obtained from the same animals which were used for the biodistribution studies. Rats were sacrificed by decapitation at 10 min p.i. of 7-^{131}I-FAUC 113 with (n=4) or without (n=6) 1mg/kg L-750667 in a volume of 50-100 µl PBS. The whole brain was removed carefully and frozen in cooled hexane at -70°C. Sagittal sections of 20 µm were cut on a cryostat microtome (HM550, Microm, Germany) at -20°C and thaw-mounted on glass microscope slides. After complete air-drying the radiolabeled sections were covered by the solid scintillator sheet for autoradiography (µ-Imager, Biospace). Anatomic images of the same slices were also obtained by the interlaced CCD of the µ-Imager system. These images were used for defining regions of interest (ROIs). The ROIs were then transferred to the autoradiographic images allowing the quantification of these brain regions by using the autoradiographic intensities (Beta-Vision Software, Biospace).

Statistics

The intensities of ROIs in autoradiographic images were obtained as cpm/mm². All experiments were performed in triplicate if not otherwise indicated. Data are expressed as mean ± SD. The significance of differences in means was examined using Student's *t* test for paired data. p values <0.05 were considered significant.

tissue / organ	injected dose (%/g)		
	5 min (n=2)	10 min (n=4)	20 min (n=3)
blood	0.276 ; 0.146	0.097 ± 0.051	0.043 ± 0.003
kidney	0.079 ; 0.055	0.603 ± 0.047	0.136 ± 0.022
liver	0.072 ; 0.040	0.357 ± 0.070	0.120 ± 0.006
lung	0.093 ; 0.029	0.422 ± 0.124	0.093 ± 0.019
heart	0.049 ; 0.029	0.204 ± 0.062	0.041 ± 0.006
spleen	not determined	0.187 ± 0.032	0.080 ± 0.009
thyroid	not determined	0.449 ; 0.343 (n=2)	not determined

Tab. 1 Blood and tissue distributions of 7-^{131}I-FAUC 113 in Sprague-Dawley rats at 5, 10 and 20 min p.i.(mean percentage ± SD values of injected dose per gram of wet tissue; independent experimental values expressed for n=2)

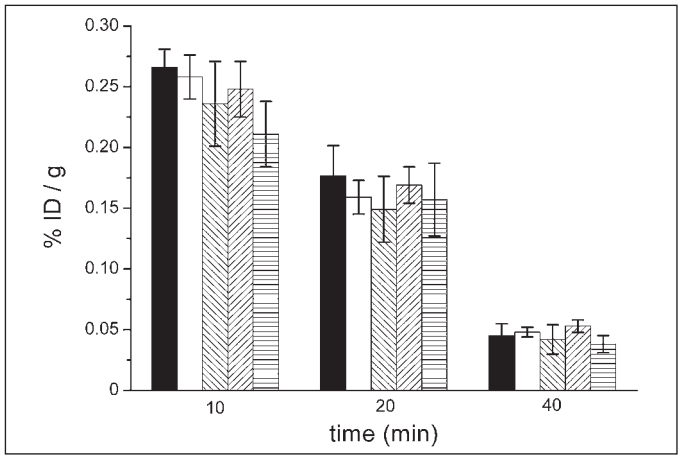

Fig. 2 Distribution of 7-^{131}I-FAUC 113 in rat brain. Uptake values are expressed as mean percentage ± SD values of the injected dose per gram of wet tissue (10 min, n=4; 20 min, n=3; 40 min, n=2). ■: frontal cortex; □: cortex; right-handed stripe: striatum; left-handed stripe: brainstem; horizontal stripe: cerebellum

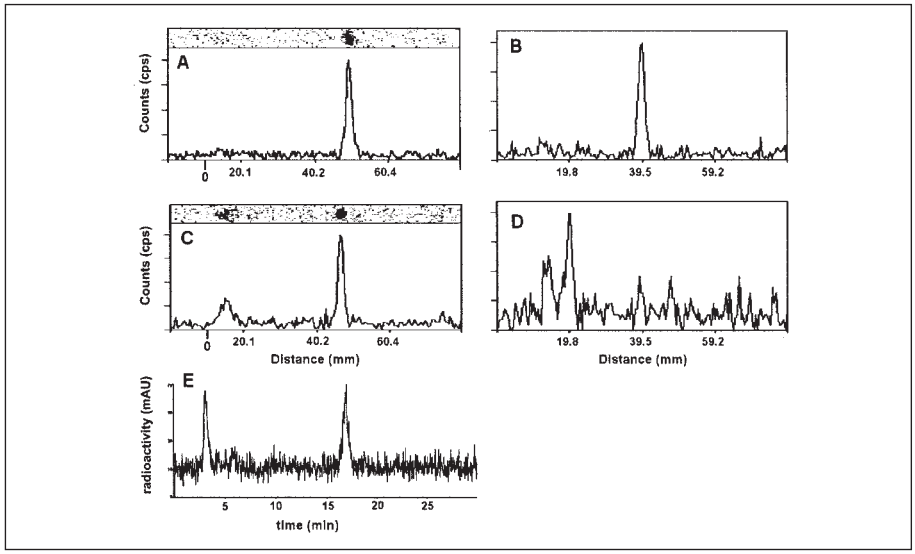

Fig. 3 Radio-tlc analysis of tissue samples after intravenous injection of 7-^{131}I-FAUC 113 (20 min p.i.)
A: control, B: frontal cortex (FC), C: liver, D: blood; E: radio-HPLC analysis of metabolites in blood (10 min p.i.)

Results

Biodistribution and brain uptake of 7-^{131}I-FAUC 113

Following intravenous injection of 7-^{131}I-FAUC 113 into Sprague-Dawley rats, the time course of radioactivity was determined in several tissues (Table 1). 7-^{131}I-FAUC 113 was rapidly cleared from the blood pool. At 10 min p.i., the highest uptake was observed for all organs under investigation. The radioactivity in the kidney was highest, from thereon decreasing, clearance via the bladder being the main degradation pathway for 7-^{131}I-FAUC 113. High uptake was also observed in the thyroid at 10 min, indicating metabolic deiodination of the tracer followed by trapping of ^{131}I-iodide. Brain uptake of 7-^{131}I-FAUC 113 revealed the highest value at 10 min p.i. for cortical areas followed by striatum, brainstem and cerebellum. For all these brain areas uptake values ranged between 0.21 and 0.26%ID/g (Fig. 2).

Lipophilicity and in vivo stability

We also determined logP for 7-^{131}I-FAUC 113 as an indicator for lipophilicity and blood-brain-permeability (logP=2.36±0.15; n=4). The in vivo stability of 7-^{131}I-FAUC 113 in tissue samples was assessed by radio-tlc and radio-HPLC at 20 min p.i. (Fig. 3). As shown in Fig. 3B, the radioactivity in the frontal cortex was referred to intact radioligand and in the liver to almost 70% of recovered radioactivity, whereas 7-^{131}I-FAUC 113 was completely absent in blood at 20 min (Fig. 3D). In accordance with that, 54% of detected radioactivity was determined to be intact radiotracer in the blood pool at 10 min p.i. (radio-HPLC, Fig. 3E).

Ex-vivo and in-vitro autoradiography

As determined by ex-vivo autoradiography, the ratio of prefrontal cortex to cerebellum (FC/CE) depicted a maximum at 10 min p.i. (1.57±0.13, n=6) and quickly decreased

within 10 min to a value of about 1 (Fig. 4). Representative sagittal brain slices for control animals and animals coinjected with the D4-antagonist L-750,677 including the white-light images for anatomical orientation are shown in Fig. 5A and Fig. 5B, respectively. For coinjected (n=4) and control animals (n=6) ratios of regions of interest (ROI) for frontal cortex to striatum (FC/ST) and frontal cortex to cerebellum (FC/CE) were determined (Fig. 6). Statistical analysis of these ratios revealed no significant difference between coinjected and control animals (Fig. 6; $p > 0.1$). In addition, we determined the dependence of regional brain uptake values on the amount of injected radiolabelled ligand in three independent animals by using a 14-20-fold increased injected dose. The analysis of ratios of ROI for these animals resulted in FC/CE=1.48±0.22 (n=3) and FC/ST=1.28±0.12 (n=3). In comparison with Fig. 6, no significant alteration was observed when increasing the injected dose. In-vitro autoradiography revealed a maximum displacement rate of 10-17% by the use of cold 7-iodo-FAUC 113, whereas the presence of the sigma receptor agonist DTG (0.5 µmol/l) and the serotonin antagonist pindolol (0.1 µmol/l) or L-750,667 (5 µmol/l) had an even weaker effect on 7-^{131}I-FAUC binding in rat brain slices (Tab. 2).

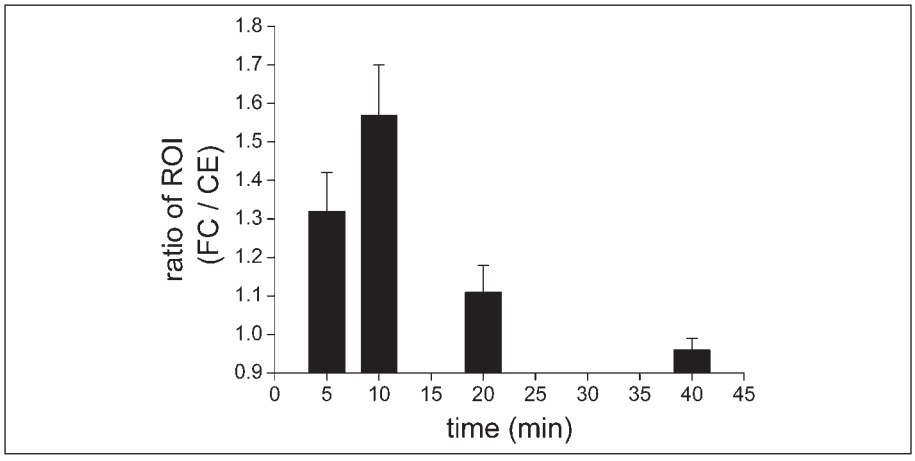

Fig. 4 Uptake ratios between frontal cortex and cerebellum after 5 min (n=3), 10 min (n=6), 20 min (n=3), and 40 min (n=2) p.i. of 7-^{131}I-FAUC 113 as determined by autoradiography (μ-Imager, Biospace). Brain regions were defined on the corresponding white light images of 20 μm brain slices and values were expressed as ratio of cpm/mm^2 ± SD by integration of regions of interest (ROI) using the software Betavision (Biospace).

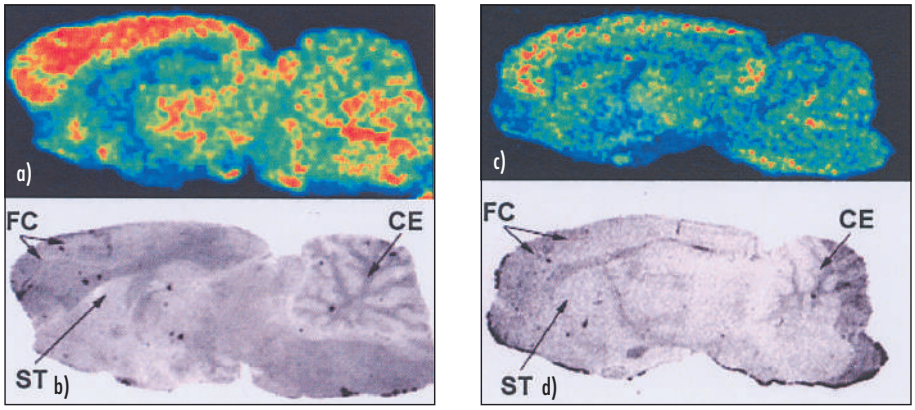

Fig. 5 Ex-vivo autoradiography (a, c) and corresponding white light image (b, d) of a representative sagittal rat brain slice (20 μm): Brain regions were defined on the white light images (FC: frontal cortex; ST: striatum; CE: cerebellum) and then transferred to the autoradiography to obtain uptake values (cpm/mm^2 ± SD) using the software Betavision (Biospace).
a, b) 10 min p.i. of 7-^{131}I-FAUC 113
c, d) 10 min p.i. of coinjected L-750667 (1 mg/kg body weight) and 7-^{131}I-FAUC 113.

Discussion

7-^{131}I-FAUC has been characterized as a radioligand with good blood-brain-permeability, rapid blood clearance and good in vivo stability using Sprague-Dawley rats. The reason for high differences in the uptake values of two animals after 5 min remained unclear, however, the main degradation pathway for 7-^{131}I-FAUC 113 was clearance via the bladder. The brain uptake of 7-^{131}I-FAUC 113 was in accordance with uptake values of established radioligands, such as ^{18}F-MPPF, a specific 5-HT$_{1A}$ radioligand (0.24 %ID/g, 15 min p.i., hippocampus) (28).

A more detailed comparison to structurally related radioligands was difficult due to limited data in the literature: Eskola et al. re-

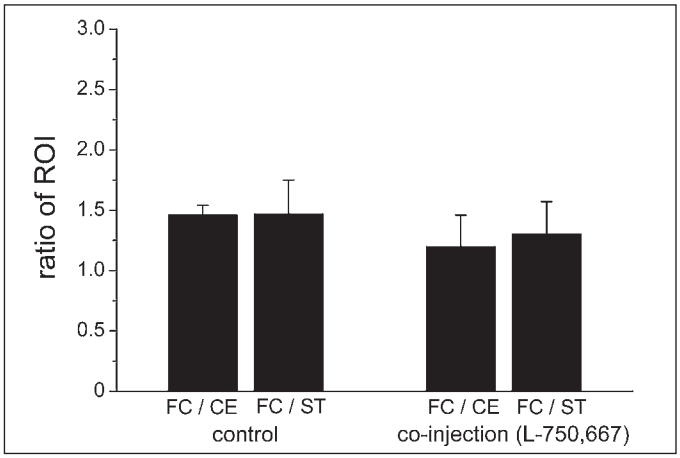

Fig. 6 Comparison of frontal cortex-to-cerebellum ratio (FC/CE) and frontal cortex-to-striatum ratio (FC/ST) of 7-^{131}I-FAUC 113 at 10 min p.i. with (n=4) and without coinjection of L-750667 (1 mg/kg body weight) (n=6). Statistical analysis showed no significant difference of mean values ($p > 0.1$).

Tab. 2 Inhibitory effect (%) on in vitro binding of 7-^{131}I-FAUC 113 to rat brain slices (20 μm) by various ligands (mean percentage of total binding ;n=3, SD <7%, 7-^{131}I-FAUC 113 binding determined as cpm/mm^2 and set as 100%)

brain region	relative uptake of 7-^{131}I-FAUC 113 (%)			
	7-^{131}I-FAUC 113	DTG (0.5 μmol/l), Pindolol (0.1 μmol/l)	L-750, 667 (5 μmol/l)	7-I-FAUC 113 (5 μmol/l)
frontal cortex	100	98	94	88
cerebellum	100	96	104	89
striatum	100	103	101	86
hippocampus	100	97	89	93
thalamus	100	97	86	83

ported uptake values of approximately 1% ID/g at 5 min p.i. in various brain regions including cortex and cerebellum for a ^{18}F-labelled pyrrolo(2,3-*b)*pyridine derivative (8). Oh et al. reported 7-9 %ID/g in mouse brain for a structurally related ^{18}F-fluoromethylbenzyl substituted pyrrolo(2,3-*b)*pyridine derivative and calculated a logP-value of 3.3 for this compound (27). In our experiment logP was 2.36 indicating a decreased lipophilicity for pyrazolo(1,5-*a)*pyridine derivatives when compared to the pyrrolo(2,3*b)*pyridine derivative described by Oh et al. However, 7-^{131}I-FAUC 113 was almost uniformly distributed in whole brain of Sprague-Dawley rats and rapidly cleared (Fig. 2).

Ex-vivo autoradiography and comparison to in-vitro results

In order to investigate the in-vivo specificity of 7-^{131}I-FAUC 113 we assessed the ratio of uptake values for distinct rat brain regions more accurately by autoradiography. This technique should yield more precise uptake values by integration of brain regions on sagittal cryo sections compared to radioactive counts obtained from dissected tissue samples of rat brain. For this purpose we used the high-performance radio-imaging method of the µ-Imager (Biospace). This device couples a thin scintillation sheet to an intensified CCD leading to significant improvement of spatial resolution for most beta-emitting isotopes, especially suited for radio-imaging of low-expression level sites (5).

The cerebellum was reported to represent an area without significant D4 receptor expression (30). Therefore, we investigated the ratio of prefrontal cortex to cerebellum (FC/CE) time-dependently by ex-vivo autoradiography. In addition, rats were coinjected with 1 mg/kg L-750667, a D4 receptor antagonist (12), in order to block putative specific binding of 7-^{131}I-FAUC 113. Since the rat striatum also represents an area of very little expression of the D4 receptor (23, 25), the frontal cortex-to-striatum ratio was additionally analysed. Statistical analysis of these ratios revealed no significant difference between coinjected and control animals. Furthermore, a 14-20-fold increased injected dose of 7-^{131}I-FAUC 113 did not induce significant alterations of tracer uptake in putative receptor-positive brain regions as indicated by a non-varying FC/CE ratio. Thus, the increased FC/CE ratio of 7-^{131}I-FAUC 113 at 10 min post injection (Fig. 4) could presumably be explained by higher regional blood flow or capillary density in the rat frontal cortex than in cerebellum, and not by specific binding of 7-^{131}I-FAUC 113. Although 7-^{131}I-FAUC 113 and the reference compound FAUC 113 showed high affinity in the in-vitro assay using membranes of transfected CHO-cells stably expressing the dopamine D4 receptor subtype (18, 29), we did not observe selective binding on native rat brain tissue samples analysed by ex-vivo autoradiography. This observation could be due to the very low D4 receptor density in rat brain reported to range between 9 and 30 fmol/mg (14, 30), so that it is reasonable to suppose that saturation of the D4 receptor could be reached with relatively low amounts of cold ligand.

The ex-vivo autoradiography data were also consistent with the in-vitro autoradiography results using 7-^{131}I-FAUC 113 (Table 2). All the agents we used for binding inhibition studies with 7-^{131}I-FAUC 113 on rat sagittal slices were ineffective, including 1,3-di-*o*-tolylguanidine (DTG, sigma receptor agonist) and pindolol (unselective serotonin antagonist), L-750667 (Fig. 1, D4 receptor antagonist) and authentic cold 7-iodo-FAUC 113 (29). These results suggest nonspecific binding of 7-^{131}I-FAUC 113. However, significant nonspecific binding of 7-^{131}I-FAUC 113 to sigma or serotonin sites can be excluded and ex-vivo autoradiography imaging also did not reveal any relevant uptake in brain regions which are untypical for D4 receptors. 7-^{131}I-FAUC 113 was rather characterized by rapid clearence from the brain.

The loss of regional specificity in blockade may also have resulted from

- low B_{max}/K_d ratio and thus low binding potential in vivo or
- saturation of the entire population of dopamine D4 receptor subtypes.

The concentration of D4 subtypes in the cortex of rat brain averages 12.4 pmol/g tissue (30). In our experiments we determined the amount of cold ligand by UV-absorbance (HPLC) detecting a maximum of 0.4 nmol refered to the sensitivity limit of UV-detection. If we assume 1 %ID/g concentrated in the brain, the localized amount of cold ligand can be estimated at 2 pmol/g ($0.01 \times 0.4 \times 10^{-9}$ mol = 2 pmol/g). In consideration of the D4 affinity of 7-^{131}I-FAUC (K_i=2.6 nmol/l) the amount of cold ligand in the brain therefore could saturate the D4 receptors significantly. However, this assumption can be extrapolated to in vivo conditions only with utmost caution, since the in vivo distribution of a radioligand at a single time point is likely to be influenced by various factors besides receptor density and affinity, such as blood flow, clearance of the radioligand and binding to nonspecific sites.

Conclusion

7-^{131}I-FAUC has been characterized as a radioligand with good blood/brain permeability and rapid blood clearance in vivo using Sprague-Dawley rats. The brain distribution of 7-^{131}I-FAUC was mainly homogeneous with the frontal cortex as exception probably due to increased blood flow in this brain area. Furthermore, the regional brain uptake of 7-^{131}I-FAUC could not be blocked by L-750667 in vivo. Therefore, together with the lack of specific D4 receptor binding in vitro, we conclude that 7-^{131}I-FAUC is not suitable for imaging of D4 receptors neither in vivo (when labelled with iodine-123) nor in vitro.

However, the relatively low specific activity could have prevented the detection of apparently low D4 receptor densities in the rat brain. Future efforts in the development of selective D4 radioligands in our laboratory are addressed to improve not only specific activity but also other characteristics, such as radiochemical yield, dopamine D4 receptor affinity and subtype selectivity or blood/brain barrier permeability.

Acknowledgement

The authors thank Mrs S. Pachaly, Mrs M. Gack and Dr. N. Thürauf for support with the rat brain slices and animal experiments. This work was supported by the ELAN-Fonds of the Friedrich-Alexander University Erlangen-Nürnberg (02.08.06.1) and by a grant from the Deutsche Forschungsgemeinschaft (DFG, PR 677/2–1).

References

1. Ariano MA, Wang J, Noblett KL et al. Cellular distribution of the rat D_4 dopamine receptor protein in the CNS using anti-receptor antisera. Brain Res 1997; 752: 26–34.
2. Bartenstein P. PET in neuroscience. Nuklearmedizin 2004; 43: 33–42.
3. Boy C, Klimke A, Holschbach M et al. Imaging dopamine D_4 receptors in the living primate brain: a positron emission tomography study using the novel D_1/D_4 antagonist [^{11}C]SDZ GLC 756. Synapse 1998; 30: 341–50.
4. Boyfield I, Brown TH, Coldwell MC et al. Design and synthesis of 2-naphthoate esters as selective dopamine D_4 antagonists. J Med Chem 1996; 39: 1946–8.
5. Charon Y, Laniece P, Tricoire H. Radio-imaging for quantitative autoradiography in biology. Nucl Med Biol 1998; 25: 699–704.
6. Defagot MC, Falzone TL, Low MJ et al. Quantitative analysis of the dopamine D_4 receptor in the mouse brain. J Neurosci Res 2000; 59: 202–8.
7. Defagot MC, Malchiodi EL, Villar MJ et al. Distribution of the D_4 dopamine receptor in rat brain with sequence-specific antibodies. Mol Brain Res 1997; 45: 1–12.
8. Eskola O, Bergman J, Lehikoinen P et al. Synthesis of 3-[[4-(4-[^{18}F]fluorophenyl)piperazin-1-yl]methyl]-1*H*-pyrrolo[2,3-*b*]pyridine. J Label Compd Radiopharm 2002; 45: 687–96.
9. Helmeste DM, Tang SW, Bunney WE et al. Decrease in sigma but no increase in striatal dopamine D_4 sites in schizophrenic brains. Eur J Pharmacol 1996; 314: R3-5.
10. Holschbach MH, Olsson RA, Bier D et al. Synthesis and evaluation of no-carrier-added 8-cyclopentyl-3-(3-^{18}F-fluoropropyl)-1-propylxanthine (^{18}F-CPFPX): a potent and selective A_1-adenosine receptor antagonist for in vivo imaging. J Med Chem 2002; 45: 5150–6.
11. Hübner H, Kraxner J, Gmeiner P. Cyanoindole derivatives as highly selective dopamine D4 receptor partial agonists: Solid-phase synthesis, binding assays, and functional experiments. J Med Chem 2000; 43: 4563–9.
12. Kulagowski JJ, Broughton HB, Curtis NR et al. 3-[4-(4-Chlorophenyl)piperazin-1-yl]methyl-1*H*-pyrrolo(2,3-*b*)pyridine: an antagonist with high affinity and selectivity for the human dopamine D_4 receptor. J Med Chem 1996; 39: 1941–2.
13. Lahti RA, Roberts RC, Tamminga CA. D2 family receptor distribution in human postmortem tissue: an autoradiographic study. Neuroreport 1995; 6: 2505–12.
14. Lahti RA, Roberts RC, Cochrane EV et al. Direct determination of dopamine D_4 receptors in normal and schizophrenic postmortem brain tissue: a [^{3}H]NGD-94–1 study. Mol Psychiatry 1998; 3: 528–33.
15. Langer O, Halldin C, Chou Y et al. Carbon-11 PB-12: an attempt to visualize the dopamine D_4 receptor in the primate brain with positron emission tomography. Nucl Med Biol 2000; 27: 707–14.
16. Lanig H, Utz W, Gmeiner P. Comparative molecular field analysis of dopamine D4 receptor antagonists including 3-[4-(4-Chlorophenyl)piperazin-1-ylmethyl]pyrazolo(1,5-*a)*pyridine (FAUC 113), 3-[4-(4-Chlorophenyl)piperazin-1-ylmethyl]-1H-pyrrolo(2,3-*b)*pyridine (L-745,870), and clozapine. J Med Chem 2001; 44: 1151–7.
17. Lidow MS, Wang F, Cao Y et al. Layer V neurons bear the majority of mRNAs encoding the five distinct dopamine receptor subtypes in the primate prefrontal cortex. Synapse 1998; 28: 10–20.
18. Löber S, Hübner H, Gmeiner P. Azaindole derivatives with high affinity for the dopamine D_4 receptor: synthesis, ligand binding studies and comparison of molecular electrostatic potential maps. Bioorg Med Chem Lett 1999; 9: 97–102.
19. Löber S, Hübner H, Utz W et al. Rationally based efficacy tuning of selective dopamine D4 receptor ligands leading to the complete antagonist 2-[4-(4-chlorophenyl)piperazin-1-ylmethyl] pyrazolo(1,5-*a*])pyridine (FAUC 213). J Med Chem 2001; 4417: 2691–4.
20. Löber S, Aboul-Fadl T, Hübner H et al. Di- and trisubstituted pyrazolo[1,5-a]pyridine derivatives: synthesis, dopamine receptor binding and ligand efficacy. Bioorg Med Chem Lett 2002; 12: 633–36.
21. Matarrese M, Soloviev D, Moresco RM et al. Synthesis and in vivo evaluation of 3-^{11}C-methyl-(3-methoxy-naphthalen)-2-yl-(1-benzyl-piperidin)-4-yl-acetate (SB-235753), as a putative dopamine D_4 receptors antagonist for PET. J Label Compd Radiopharm 2000; 43: 359–74.
22. Matulenko MA, Surber B, Fan L et al. Synthesis and activity of 2-[4-(4-^{3}H-2-cyanophenyl)piperazinyl]-N-(2,4,6-^{3}H-3-3-methylphenyl)acetamide: a selective dopamine D4 receptor agonist and radioligand. Bioorg Med Chem Lett 2004; 14: 5095–8.
23. Meador-Woodruff JH, Damask SP, Wang J et al. Dopamine receptor mRNA expression in human striatum and neocortex. Neuropsychopharmacology 1996; 15: 17–29.
24. Mrzljak L, Bergson C, Pappy M et al. Localisation of dopamine D_4 receptors in GABAergic neurons of the primate brain. Nature 1996; 381: 245–8.
25. O'Malley KL, Harmon S, Tang L et al. The rat dopamine D4 receptor: sequence, gene structure, and demonstration of expression in the cardiovascular system. New Biol 1992; 4: 137–46.
26. Oak JN, Oldenhof J, Van Tol HHM. The dopamine D_4 receptor: one decade of research. Eur J Pharmacol 2000; 405: 303–27.
27. Oh SJ, Lee KC, Lee SY et al. Synthesis and evaluation of fluorine-substituted 1*H*-pyrrolo 2,3-*b*-pyridine derivatives for dopamine D_4 receptor imaging. Bioorg Med Chem 2004; 12: 5505–13.
28. Plenevaux A, Weissmann D, Aerts J et al. Tissue distribution, autoradiography, and metabolism of 4-(2'-methoxyphenyl)-1-[2'-(N-2"-pyridinyl-p-^{18}F-fluorobenzamido)ethyl]piperazine (p-^{18}F-MPPF), a new serotonin 5-HT_{1A} antagonist for positron emission tomography: An in vivo study in rats. J Neurochem 2002; 75: 803–11.
29. Prante O, Löber S, Hübner H et al. Synthesis and in vitro evaluation of iodine labelled pyrazolo(1,5-*a*)pyridines as highly selective dopamine D4 receptor ligands. J Label Compd Radiopharm 2001; 44: 849–58.
30. Primus RJ, Thurkauf A, Xu J et al. Localization and characterization of dopamine D_4 binding sites in rat and human brain by use of the novel, D_4 receptor-selective ligand ^{3}H-NGD 94–1. J Pharmacol Exp Ther 1997; 282: 1020–7.
31. Reynolds GP, Mason SL. Absence of detectable striatal dopamine D_4 receptors in drug-treated schizophrenia. Eur J Pharmacol 1995; 281: R5-R6.
32. Seeman P, Guan HC, Van Tol HHM. Dopamine D_4 receptors elevated in schizophrenia. Nature 1993; 365: 441–5.
33. Staley JK, Tamagnan G, Baldwin RM et al. SPECT imaging with the D_4 receptor antagonist L-750667 in nonhuman primate brain. Nucl Med Biol 2000; 27: 547–56.
34. Van Tol HHM, Bunzow JR, Guan HC et al. Cloning of the gene for a human dopamine D_4 receptor

with high affinity for the antipsychotic clozapine. Nature 1991; 350: 610–4.
35. Wong AHC, Van Tol HHM. The dopamine D4 receptors and mechanisms of antipsychotic atypicality. Prog Neuropsychopharmacol Biol Psychiatry 2003; 27: 1091–9.
36. Zhang MR, Haradahira T, Maeda J et al. Syntheses and pharmacological evaluation of two potent antagonists for dopamine D_4 receptors: ^{11}C-YM-50001 and N-2-[4-(4-chlorophenyl)piperazin-1- yl]ethyl-3-^{11}C-methoxybenzamide. Nucl Med Biol 2002; 29: 233–41.

Correspondence to:
Olaf Prante, PhD
Labor für Molekulare Bildgebung, Nuklearmedizinische Klinik
Friedrich-Alexander Universität Erlangen-Nürnberg
Schwabachanlage 6, 91054 Erlangen, Germany
Tel. +49/(0)91 31/85 34-440, Fax -325
E-mail: olaf.prante@nuklear.imed.uni-erlangen.de